A Grid-Connected Solar Photovoltaic System with Predictive Control Strategies considering PSO-MPPT

Yousra Izgheche*‡, Tahar Bahi‡**, Amira Lakhdara***

*Badji Mokhtar-Annaba University, Electronic Department, LASA Laboratory, Algeria

**Badji Mokhtar-Annaba University, Electrical Department, LASA Laboratory, Algeria

***Badji Mokhtar-Annaba University, Electrical Department, Algeria

(yousra.izgheche@univ-annaba.dz, tahar.bahi@univ-annaba.dz, amira.lakhdara@univ-annaba.dz)

‡Corresponding Author, Yousra Izgheche, Tahar Bahi, Badji Mokhtar-Annaba University, LASA Laboratory, 23000, Algeria,

Received: 05.10.2023 Accepted: 12.12.2023

Abstract- Control techniques have become an indispensable solution for electric power producers aiming to inject energy cleanly into traditional distribution networks while complying with current regulations and standards. Specifically, the connection of photovoltaic power plants to the grid is permitted only when specific quality and stability requirements are satisfied. This work contributes to this context by proposing control strategies for essential and unavailable static power converters to connect a photovoltaic system to a three-phase electrical network. The proposed approach employs the particle swarm optimization metaheuristic algorithm with a quadratic criterion-based objective function to control the boost converter for maximum power point tracking of the electric power produced by the photovoltaic generator. The objective is to compare two control strategies to identify the most effective approaches to deliver superior quality and performance. The results obtained demonstrate that the current predictive control strategy utilizing a finite control set model is preferable for selecting the optimal switching state applied to the three-phase three-level inverter, providing superior control performance compared to the alternative voltage-oriented control strategy. Voltage-oriented control and finite control set model predictive control current commands are recommended to select the optimal switching state for the three-level three-phase inverter. Finally, the overall energy conversion chain with the proposed new control configuration is subjected to testing under varying weather conditions, and the analysis of results validates the effectiveness of the adopted approach.

Keywords Renewable energy, MPPT, particle swarm optimization, voltage oriented control, model predictive control.

1. Introduction

Since the industrial revolution, global final energy consumption has been steadily increasing, with particularly rapid growth in emerging countries. However, even though the International Energy Agency (IEA) reports a slight decline in the share of fossil fuels, including the top three sources of supply: petroleum, coal, and natural gas, they still dominate the global primary energy mix [1]. Fossil fuels account for about two-thirds of final consumption on all continents, with this consumption mainly relying on petroleum products, about 20% of which are used for electricity production [2]. For decades, electricity production from fossil fuels has been one of the primary and essential sources of energy for humanity. However, over time, it has become clear that the technology used for electricity production has its disadvantages and limitations. One primary drawback associated with the utilization of fossil fuels for electricity generation is their adverse environmental impact. The combustion of these fossil fuels releases greenhouse gases, which play a significant role in contributing to climate change, and their extraction, transportation, and combustion have detrimental effects on the environment, including air, water, and soil pollution. Another major disadvantage of using fossil fuels is their depletion. Fossil fuel reserves are non-renewable and will inevitably run out in the near future. Furthermore, extracting these fuels is becoming increasingly difficult and costly as the easy-to-exploit reserves diminish [3, 4]. As an alternative to fossil fuels, the world is increasingly turning to renewable

energy (RE), including solar, wind, hydro, geothermal, and biomass energy, thanks to their exceptional potential and advantages for effectively ensuring the energy transition. The benefits of using RE are numerous, including reducing greenhouse gas emissions, long-term sustainability, energy security, and independency [5]. As a result, the increasing use of renewable energy sources in the electricity system has become a significant trend. Statistics show a gradual decline in the use of fossil fuels and a rapid deployment of solar systems, indicating that soon this energy source will dominate the renewable energy market, which is a good indication that the energy transition is underway. However, the results are still inadequate, and the question of the development of RE and the necessary investments in the field is still the question of the day [6-8].

This work focuses on solar energy (SE), which is one of the most abundant and unlimited sources of renewable energy for humanity. It is available everywhere and free of charge, even for individual users, thanks to solar panels. Its use to produce electricity is emission-free and pollution-free, contributing to energy independence and community resilience. Solar energy is currently exploited through two major technological pathways: thermal and photovoltaic (PV). The thermal pathway converts solar radiation into thermal energy, allowing, among other things, the production of electricity, heat, or cold. On the other hand, the photovoltaic pathway directly converts solar radiation into electricity [9].

Due to system constraints caused by the external environment and grid faults, conventional methods of maximum power point tracking (MPPT) and inverter control of a photovoltaic power generation system cannot achieve optimum power. Photovoltaic installations connected to the electrical distribution grid enable the production of electricity from solar energy and supply it to the electrical grid. They are generally composed of a photovoltaic generator (PVG) that transforms solar energy into direct current (DC) voltage, which is then used to power the input of a DC/DC converter (chopper) that, in turn, provides an appropriate DC voltage to power a three-phase inverter to convert it into alternating current (AC). The electricity can then be used directly by local consumers or, in case of excess, injected into the electrical grid or stored in an energy storage system for later use according to predefined conditions [10-12]. However, several challenges persist that need to be addressed to ensure effective integration of photovoltaic installations into the grid. These challenges mainly include managing the intermittent production of solar energy depending on weather conditions, which requires updating the control and energy management configurations to ensure the required reliability of the PV system's connection to the grid under all atmospheric conditions. Therefore, this work proposes the use of the particle swarm optimization (PSO) metaheuristic algorithm with a quadratic criterion-based objective function to control a boost converter to extract maximum electrical power and voltage-oriented control (VOC) and finite control set model predictive control current (MPC) commands to control a three-level three-phase inverter and manage active and reactive power [13-16]. Finally, the overall system's operation with the recommended new control configuration is subjected to testing under varying weather conditions, and the analysis of results validates the effectiveness of the adopted approach.

2. System Description

Photovoltaic installations connected to the electrical distribution grid constitute a significant part of photovoltaic installations worldwide. They are generally composed of a set of solar panels connected in series or parallel to form a PVG that powers a chopper to adjust its output voltage with the required input voltage to connect to an inverter, which is then connected to the distribution or transmission electrical grid. The excess of energy produced by these installations is sold and injected into the electrical grid, and when the owner of such an installation needs electrical energy, they can be supplied with electricity from the grid to which it is connected at the purchase price. Therefore, the PVG-grid connection compensates for differences between production and consumption without the need for a battery storage system, no energy is lost, the storage system is not required, the surplus energy produced by the PVG is billed, and the installation owner is assured of having energy even if weather conditions (irradiation and temperature) are unfavorable. Indeed, due to the variable nature of PVG power, additional power regulation is necessary. The most common methods for extracting the maximum power produced (MPPT) are the perturbation and observation (P&O) method and the incremental conductance (INC) method, but these methods have poor performance when atmospheric conditions change rapidly or under partial shading conditions where the P=f(V) curve has several maxima [17-20].

The configuration considered in this work essentially includes: a PVG that transforms solar irradiation into direct current, a power converter (boost chopper) controlled by a maximum power point tracking (MPPT) block based on the PSO algorithm to increase the voltage level provided at the output of the PVG to a required DC voltage level at the input of a three-level inverter that transforms the DC current into AC current controlled by MPC, a filter, and a three-phase distribution network, as shown in Figure 1. The AC current established by the inverter is either used by local loads or injected into the distribution network [21].

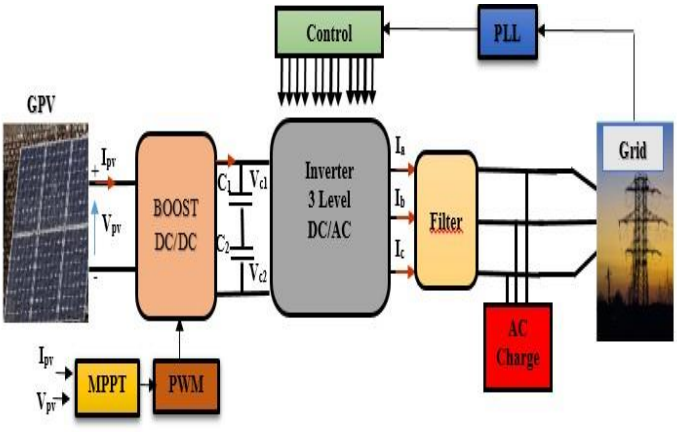

Fig. 1. System structure.

3. Design and Modeling

3.1. Modeling of PV Cells

Photovoltaic cells are basic semiconductor elements used to create solar panels and photovoltaic generators. They convert light into electrical energy through the photovoltaic effect and are typically arranged in series and parallel to form a solar panel. However, according to the literature, a single-diode electrical circuit as shown in Figure 2 is often used to model a silicon photovoltaic cell and simulate its behavior [22]. This model consists of a photocurrent source, a non-linear diode, a series resistor that represents internal losses, and a resistor connected in parallel with the diode to account for leakage current to the ground.

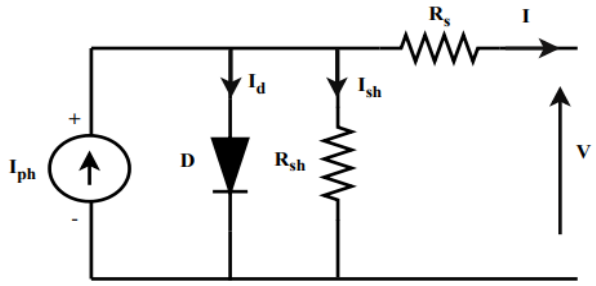

Fig. 2. Electrical circuit equivalent of a GPV cell.

From this circuit, we can deduce the following expressions [23, 24]:

$$I_{pv} = I_{ph} - I_d - I_{sh} \quad (1)$$

The current through these elements is governed by the voltage across them:

$$V_d = V_{pv} + I_{pv}R_s \quad (2)$$

By the Shockley diode equation, the current diverted through the diode is:

$$I_d = I_0[e^{(\frac{q V_d}{nkT})} - 1] \quad (3)$$

By Omh's law, the current diverted through the shunt resistor is:

$$I_{sh} = \frac{V_d}{R_{sh}} \quad (4)$$

$$I_{pv} = I_{ph} - I_0[e^{(\frac{q(V_{pv}+I_{pv}R_s)}{nkT})} - 1] - \frac{V_{pv}+I_{pv}R_s}{R_{sh}} \quad (5)$$

Where, I_{ph} :photocurrent; I_0 : reverse saturation current; I_{pv}: cell output current; V_d: voltage across diode ; V_{pv} : cell's output voltage; R_s :serie resistance; R_{sh} : shunt resistance; N_s : number of cells in one module; n : diode ideality factor; k :Boltzmann's constant (1.381×10^{-23}) ; T: absolute temperature equals -273.15°C and q : electron charge (1.602×10^{-19}C).

The model described above was implemented using MatLab/Simulink software, taking into account the given parameters in Table 1.

Table 1. Parameters of the GPV

GPV's characteristics	Value
Maximum Power (P_{mp})	100 kW
Cells per module (N_{cell})	60
Open circuit voltage (V_{oc})	36 V
Short-circuit current (I_{sc})	7.8 A
Voltage at Maximum power point (V_{mp})	345 V
Current at Maximum power point (I_{mp})	290 V

Next, the system was tested for 4 levels of solar irradiation (1000W/m^2 (standard), 700W/m^2, 500W/m^2, and 300W/m^2) while maintaining a constant temperature of 25°C. Figure 3 illustrates the current and power characteristic curves plotted as a function of the voltage of the PV array, respectively represented by I=f (V) and P=f (V).

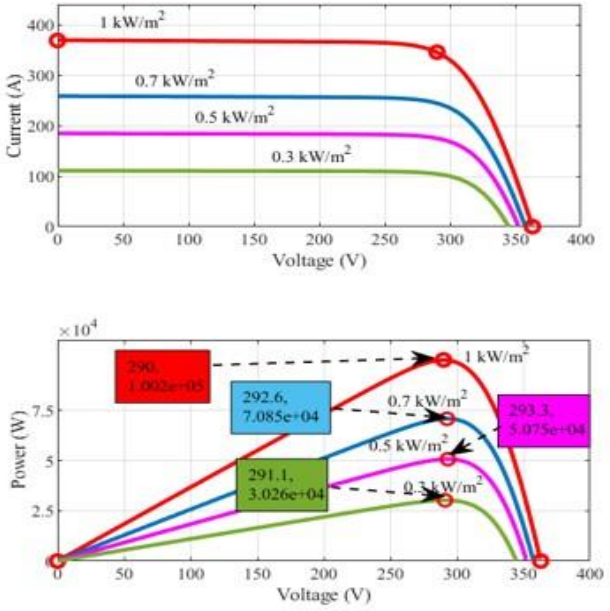

Fig. 3. I=f (V) and P=f (V) for different irradiances.

It is important to note that the photovoltaic panel exhibits nonlinear voltage-current characteristics and that there is only one operating point at which the photovoltaic system operates at maximum power output as shown in Figure 3. Therefore, in order to ensure operation at maximum power, it is necessary to implement a control system for monitoring the Maximum Power Point (MPP), which will be discussed later in this work. Additional information on this topic is provided in Table 2.

Table 2. I_{cc} and P_{pv}_Max under different irradiations

Irradiation w/m^2	I_{cc}(A)	P_{pv} _Max (w)
300	110.00	3.026e+04
500	185 .00	5.075e+04
700	258.50	7.085e+04
1000	369.20	1.002e+05

3.2. Design and Modeling of the Boost

The electrical circuit of the boost DC/DC converter is illustrated in Figure 4. Its role is to increase the low voltage at the output of the PVG to an appropriate level corresponding to the maximum power developed, and it is essentially composed of an input source voltage (V_i) representing the PVG output voltage, a boost inductor (L), an IGBT semiconductor, a boost diode (D), a capacitor (C_2) as a boost filter that reduces high-frequency harmonics, and a resistance (R) that represents the load.

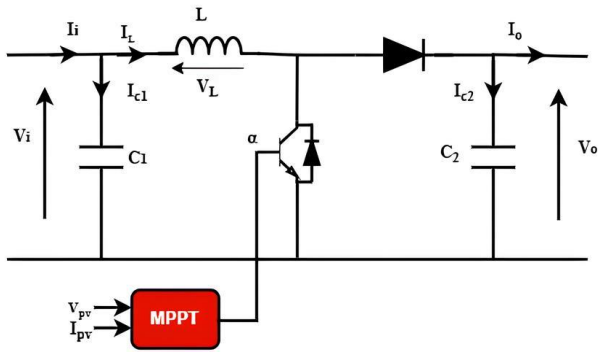

Fig. 4. Schematic circuit of the boost converter.

The IGBT semiconductor of the chopper is controlled by the duty cycle (α), with the relationship between the output voltage (V_o) and input voltage (V_i) defined by the following equation: [25]:

$$\frac{V_o}{V_i} = \frac{1}{1-\alpha} \tag{6}$$

To design such a converter, mathematical expressions given by the relations below are used, and the parameter values are presented in Table 3 [26]:

$$\alpha = 1 - \frac{V_o}{V_i} = 1 - \frac{501}{293} = 0.7098 \tag{7}$$

$$L = \frac{V_o(V_i - V_o)}{\Delta I_l * f_s * V_o} = \frac{\alpha(1-\alpha)^2}{2 * f_s} \tag{8}$$

$$C = \frac{\alpha}{R_o * f_s * \left(\frac{\Delta V_o}{V_o}\right)} = \frac{\alpha}{f_s * 0.01} \tag{9}$$

Table 3. Boost parameters

System parameters	Values
DC link capacitor	C_1 = 1mF, C_2 = 3.227 mF
Input inductor	L = 61.45 mH
Sampling period	T_s = 0.1µs
Switching frequency of switches	F_s = 100 kHz
Intput Voltage	V_i = 293 V
Output Voltage	V_o = 501 V

For this task, the duty cycle (α) is determined by the MPPT control system. It constantly switches between "Closed" and "Open" states, which correspond respectively to the values "0" and "1" during each period (T_s) of a switching cycle. Therefore, considering these two phases, we determine the corresponding mathematical models for the two possible operating configurations:

When the IGBT is closed:

$$\begin{cases} L\frac{dI_{pv}}{dt} = V_{pv} = V_l \\ C\frac{dV_{pv}}{dt} = I_{dc} = I_c \end{cases} \tag{10}$$

When the IGBT is open:

$$\begin{cases} L\frac{dI_{pv}}{dt} = V_{pv} - V_{dc} = V_l \\ C\frac{dV_{pv}}{dt} = I_{dc} - I_{pv} = I_c \end{cases} \tag{11}$$

3.3 Design and Modeling of the NPC Inverter

Figure 5 shows the structure of a three-level three-phase voltage inverter [27]. It consists of three arms and two sources of DC voltage. Each arm has four switches in series and two middle diodes. Each switch is composed of a transistor and a diode mounted head-to-tail. The DC voltage applied by the PV generator at its input as well as the switching states of all its semiconductor components must be controlled in an appropriate manner to ensure both the tracking of the reference voltage required at the DC bus level (input of the inverter) and the minimum of harmonics of the output voltages feeding the load or injected into the distribution network.

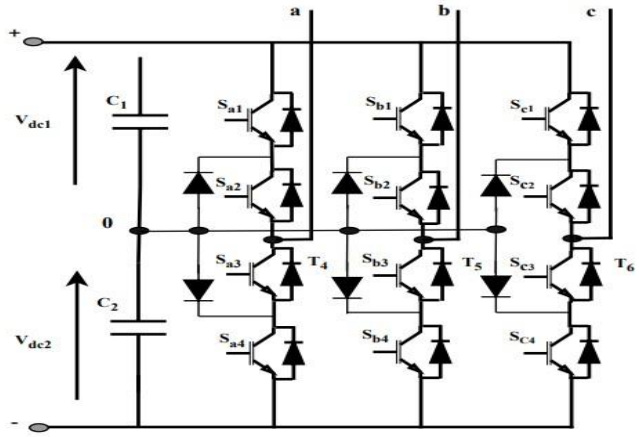

Fig. 5. Structure of the three-level inverter circuit.

Since the three-level inverter is symmetric, the study can be limited to the operation of a single arm. However, the analysis of the different operating configurations of an arm shows that out of the 24 = 16 possible configurations, only three configurations are practically possible for implementation (Sij=1100, Sij=0110, and Sij=0011) as shown in Table 4, and all other sequences are not functional and should be avoided because they either cause short circuits of the DC voltage sources or disconnect the load.

The analysis of the different possible configurations shows that the combination of three states 1, 0, and -1 produces 27 switching states, including 19 space voltage vectors for the three-phase three-level inverter. The switching states and their orientations are represented by Figure 6 [28, 29].

Table 4. Switching states of the 3-level NPC converter

Switch status				Vi
1	1	0	0	Vpv/2
0	1	1	0	0
0	0	1	1	-Vpv/2

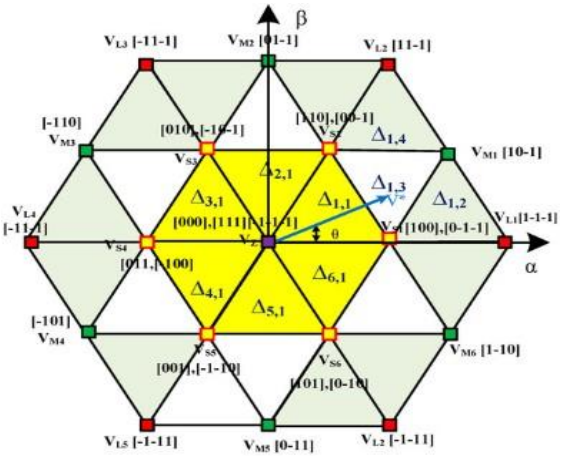

Fig. 6. Three-level inverter space vector diagram

The prediction of the output load current for the system is given by the following expression:

$$L\frac{di}{dt} = V - Ri - e \tag{12}$$

Where R and L are the load resistance and inductance respectively, v is the voltage vector generated by the inverter, and e is the electromotive force of the load, and i is the load current vector. The current and voltage vectors are defined by:

$$v = \frac{2}{3}(V_{a0} + aV_{b0} + a^2V_{c0}) \tag{13}$$

$$i = \frac{2}{3}(i_a + a_b + a^2 i_c) \tag{14}$$

$$e = \frac{2}{3}(e_a + ae_b + a^2 e_{c0}) \tag{15}$$

With, $\alpha = e^{j(\frac{2\pi}{3})}$ (16)

Regarding the filter at the output of the inverter, it is used as the interface between the inverter and the power grid. With a perfectly designed filter, a high-quality grid current can be achieved [30]. Therefore, the design requires the following parameters:

$$C_f = \frac{0{,}05P_n}{2\pi f_g V_g} \tag{17}$$

$$L_f = \frac{0{,}1V_g^{\ 2}}{2\pi f_g P_n} \tag{18}$$

Where, P_n : nominal output power, Vg : Inverter phase to phase RMS voltage, f_g : grid frequency and f_s : switching frequency.

4. Control Strategies

4.1. Array MPPT with Particle Swarm Optimization

The objective of adopting this approach is to extract the maximum value of irradiation. To achieve this, the MPPT control is implemented using the PSO algorithm [31]. Particle Swarm Optimization (PSO) is a technique inspired by the social behavior of animals that move in swarms, such as fish that move in schools or migratory birds. PSO is a stochastic optimization algorithm that moves a swarm of "particles" to search the solution space and find the optimal solution.

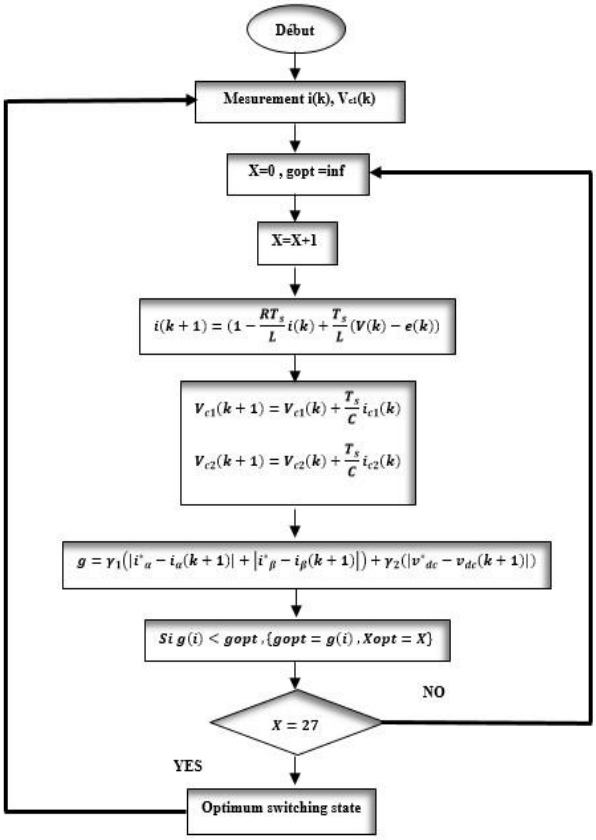

Fig. 7. Algorithm of the PSO optimization method.

The movement of each particle is influenced by its velocity and position vectors in order to reach the global optimum. The quality of its position is determined by the value of the objective function (F). In this work, we will use as the optimization criterion to be minimized a quadratic criterion expressed by the following relation:

$$F = \int_0^t e^2 dt = \int_0^t (P_o - P_i)^2 dt \tag{19}$$

Where: Po is the output power and Pi is the input power (power of the PV generator). The movement of each particle in the search space is based on its current position and the

update of its velocity. In fact, at iteration k+1, the position vector is calculated from the following equation [32, 33]:

$$V^{(k+1)}{}_i = w^* V^{(k)}{}_i + C_1 * rand(x) * \left(Pbest_i - K^{(k)}{}_i\right) + C_2 * rand(x) * \left(Gbest_i - K^{(k)}{}_i\right) K^{(k+1)}{}_i = K^{(k)}{}_i + V^{(k+1)}{}_i \quad (20)$$

Table 5. Parameters of algorithm PSO

	Symbol	Values
Number of swarm	swarms	10
Number of iterations	Iter-max	20
Weight of local information	C_1	1.6
Weight of global information	C_2	2.5
Weight of inertia	w	0.4
Dimension of the problem	Dim	1

4.2. Principle of the VOC control

The most widely recognized method for regulating active and reactive power in grid-connected applications is known as "VOC".

The diagram illustrated in Figure 8 depicts the synchronous frame VOC, which is a control scheme designed to regulate the grid current id-iq to their respective references. The reference current id is estimated using a DC-link voltage controller, while the iq reference current is estimated based on the reactive power requested by the grid operator. The measured grid currents are transformed from the natural frame (abc) to the rotating frame, and their values of id-iq are compared with their corresponding references values. Subsequently, PI-based controllers generate the d and q components of the reference voltage, which are then transferred to the αβ frame and given to the modulation stage. This control scheme, like the stationary frame VOC scheme, ensures operation at a fixed switching frequency and is easy to implement in practice. However, it has a slow response time, large current fluctuations, and significant lower-order harmonics.

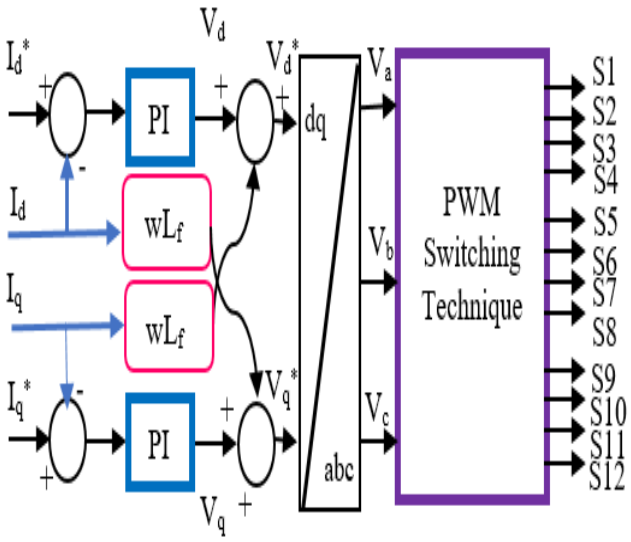

Fig. 8. Schematic diagram of the VOC technique.

Three-phase line voltages and phase current equations for grid-tied inverter are given as,

$$V_a = V_m \cos(\omega t)$$
$$V_b = V_m \cos(\omega t - 2\pi/3) \quad (21)$$
$$V_c = V_m \cos(\omega t + 2\pi/3)$$

$$I_a = I_m \cos(\omega t)$$
$$I_b = I_m \cos(\omega t - 2\pi/3) \quad (22)$$
$$I_c = I_m \cos(\omega t + 2\pi/3)$$

The topology of grid-tied inverter with LC filter is shown in figure 4 in which V_a, V_b, V_c are voltages at inverter end and U_a, U_b, U_c are voltages at grid end. By using Kirchhoff's voltage law:

$$V_a = \frac{LdI_a}{dt} + U_a$$
$$V_b = \frac{LI_b}{dt} + U_b \quad (23)$$
$$V_c = \frac{LdI_c}{dt} + U_c$$

Where, L is the inductance value of filter and I_a, I_b, I_c are values of current.

Three-phase electrical current (I_{abc}) and voltages (V_{abc}) are transformed into two phase synchronous rotating frame (SRF) dq0 system using Park's transformation (V_{dq0} and I_{dq0}). According to this transformation:

$$\begin{bmatrix} d \\ q \\ 0 \end{bmatrix} = \frac{2}{3} \begin{bmatrix} \cos\omega t & \cos(\omega t - 2\pi/3) & \cos(\omega t + 2\pi/3) \\ -\sin\omega t & -\sin(\omega t - 2\pi/3) & -\sin(\omega t + 2\pi/3) \\ 0 & 0 & 0 \end{bmatrix} \begin{bmatrix} a \\ b \\ c \end{bmatrix} \quad (24)$$

Transforming these three-phase voltage quantities into *dq* transform equation 1 can be written as,

$$V_d = \frac{LdI_d}{dt} + U_d - \omega L I_q$$
$$V_q = \frac{LI_q}{dt} + U_q + \omega L I_d \quad (25)$$

Apparent power can be presented as:

$$S = \frac{3}{2}(V_{dq} I^*{}_{dq}) \quad (26)$$

Where, I^*_{dq} is the complex conjugate of I_{dq}. Hence active and reactive powers supplied to the grid are as follows:

This technique essentially involves aligning the grid voltage with the direct axis of the rotating reference frame (d-q). This allows for the decoupling of active and reactive power, which can be controlled separately using the following expressions [34]:

$$P = \frac{3}{2}(v_d i_d) \quad (27)$$

$$Q = -\frac{3}{2}(v_d i_q) \quad (28)$$

This way, active power management is ensured by directly controlling the direct axis current (id), while reactive power regulation is achieved by using the quadrature axis current (i_q). To achieve energy balance, the direct axis current is typically drawn from the DC-link, while the quadrature axis current is set to zero for unity power factor operation. However, by adjusting the value of the quadrature axis current, it is possible to inject and support the system with reactive power, which reduces the value of active power to prevent overloading of the inverter.

To implement the VOC strategy, a cascaded loop structure is used with PI controllers. In this case, the outer loop provides the reference currents for the inner loop, which then calculates the reference voltage and applies it to the modulation stage.

4.3. Technique of FCS-MPC

The Finite Control Set Model Predictive Control Current (FCS-MPCC) uses a heuristic method to select the optimal switching state from finite candidates. This selection is made by minimizing the objective function of the problem formulation. In this study, the basic formulation of the problem is examined in detail to highlight the variable switching frequency property of FCS-MPC [35].

$$\frac{dX}{dt} = \frac{X(k+1)-X(k)}{T_s} \tag{29}$$

$$i(k+1) = (1-\frac{R_f T_s}{L_f})i(k) + \frac{T_S v(k) - e(k))}{L} \tag{30}$$

$$i_\alpha(k+1) = (1-\frac{R_f T_s}{L_f})i_\alpha(k) + \frac{T_s v_\alpha(k)}{L_f} - e_\alpha(k)) \tag{31}$$

$$i_\beta(k+1) = (1-\frac{R_f T_s}{L_f})i_\beta(k) + \frac{T_s v_\beta(k)}{L_f} - e_\beta(k)) \tag{32}$$

$$\begin{cases} i_\alpha(k+1) = i_\alpha + \frac{T_s}{L}\left(S_{ah}(k)V_{c1} + S_{al}(k)V_{c2}(k) - i_\alpha(k)R - e_\alpha(k)\right) \\ i_\beta(k+1) = i_\beta + \frac{T_s}{L}\left(S_{\beta h}(k)V_{c1} + S_{\beta l}(k)V_{c2}(k) - i_\beta(k)R - e_\beta(k)\right) \\ v_{dc}(k+1) = \frac{T_s}{c}(2i_{dc} - (S_{ah}(k) + S_{al}(k))i_\alpha(k) - (S_{bh}(k) + S_{bl}(k))i_\beta(k)) \end{cases} \tag{33}$$

The cost function serves as the selection criterion for the optimal switching signal. In this work, the cost function for the Neutral Point Clamped (NPC) inverter is defined as follows:

$$g = \gamma_1\left(|i^*{}_\alpha - i_\alpha(k+1)| + |i^*{}_\beta - i_\beta(k+1)|\right) + \gamma_2(|v^*{}_{dc} - v_{dc}(k+1)|) \tag{34}$$

Figure 9 shows the functional diagram of the FCS-MPC controller with the basic problem formulation. A three-level three-phase voltage source converter is used as the Grid-Connected Inverter (GCI), regulating the line current i_{abc} to synchronize with the grid voltage e_{abc} and transmit all real power. The regulation of the DC bus voltage V_{dc} is also added but does not affect the problem formulation in the FCS-MPC.

The FCS-MPC controller selects the optimal switching state and sends the outputs directly to the grid control circuit without a modulation process. This results in indefinite switching transitions and a variable switching frequency.

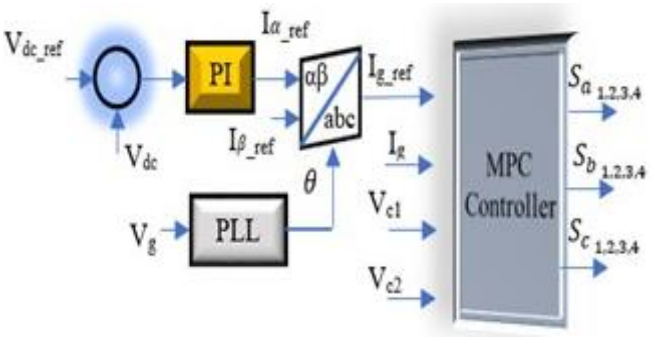

Fig. 9. FCS-MPC controller block diagram

The algorithmic structure of FCS-MPCC for PV inverters is illustrated in Figure 10. The details of the control strategy mainly include the following six parts:

Measurement module: Real operating data is sent to the system with real-time measurements of grid voltage, inverter current, and DC-link voltage. The real operating data, including DC-link voltage, is transmitted to the predictive model.

PLL: The PLL provides the coordinate transformation and phase angle of the transformation for the predictive model calculation.

Predictive model: The predictive model uses the recursive relationship described in equation (33) to compute the current predicted value at time k+1 based on the system measurements at time k.

Optimization: The square error between the reference current and the predicted current at time k+1 is used as the optimization objective function in equation (34).

Current reference: The active current reference is provided by an external continuous voltage loop. The PV module reference voltage V_{dc_ref} is generated by the MPPT controller and compared to the measured DC bus voltage V_{dc} by the MPPT controller. The PV module reference voltage V_{dc_ref} is generated by the MPPT control and compared to the measured DC bus voltage V_{dc} before being sent to the PI controller. To connect to the grid with unity power factor, the reactive current must be controlled with a PI controller. When the power factor is 1, the reactive current reference is set to 0.

The corresponding switching state for the minimum value of the optimization objective function is extracted as the optimal switching state for the next sampling period, and the semiconductor device is switched accordingly. The duration of the next samples and power semiconductor devices are switched accordingly.

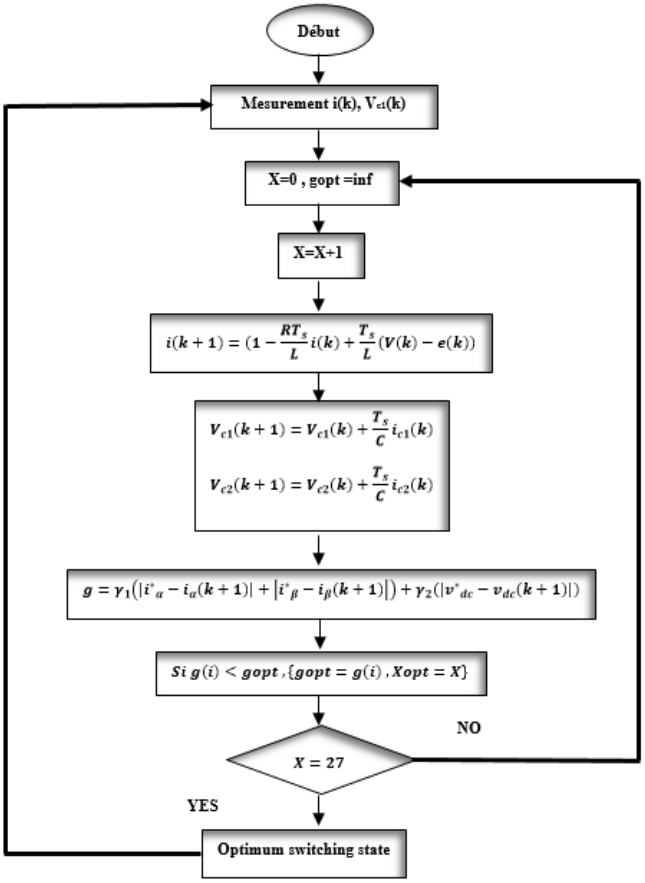

Fig. 10. Algorithm of the MPC

5. Results and Discussion

The objective of this section is to analyses and evaluate the performance of the system under consideration, particularly in diverse weather conditions. The analysis is based on four irradiance levels, serving as the foundation for this assessment. The corresponding current-voltage and power-voltage characteristics $I = f(V)$ and $P = f(V)$ are shown in Figure 3, respectively. Using the system operating at the maximum power point corresponding to the naturally imposed emission level. The tests were carried out with the irradiation profile shown in Figure 11 below:

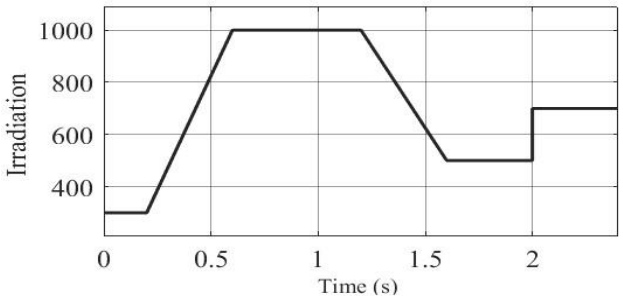

Fig. 11. Irradiation profile.

Furthermore, upon comparison with Figure 3 in Section 2, the power generated by the GPV depicted in Figure 12 aligns well with the corresponding irradiance levels. This confirmed that the system would work properly with the maximum power generated by his GPV. Indeed, the load power shown Figure 13 shows that the active power correctly follows the slot imposed by the solar radiation profile. On the other hand, the reactive power obtained from both methods, VOC and FCS-MPCC, is nearly negligible. Hence the unitary power factor. Figure 14 displays the reactive power consumed in the distribution network. It constantly fluctuates around zero it consistently fluctuates around zero, favoring systems that operate at unity power factor. Finally, Figure 15 clearly shows that the DC bus voltage perfectly follows the reference value imposed on the input voltage of the inverter, thanks to the voltage regulation provided and the result. Figure 16 shows the phase 'a' currents and their zooms obtained with both techniques. It is noteworthy that the results obtained with MPC exhibit less oscillation and demonstrate faster response times to changes. This serves as evidence of the superior performance of MPC.

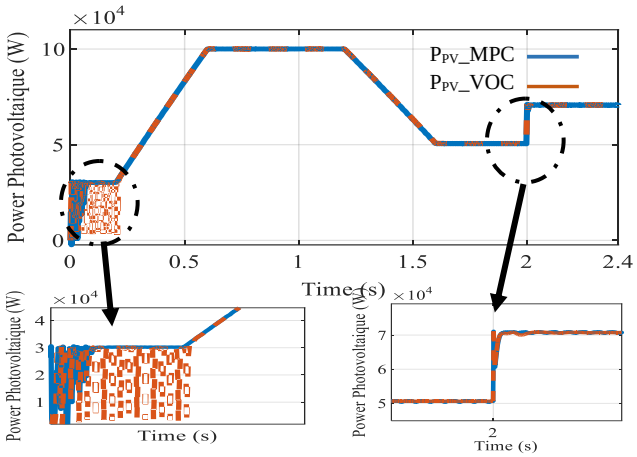

Fig . 12. Photovoltaic power with VOC and FCS-MPCC

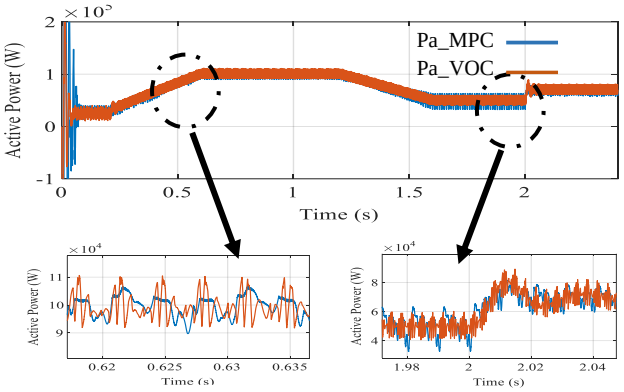

Fig. 13. Active power with VOC and FCS-MPCC.

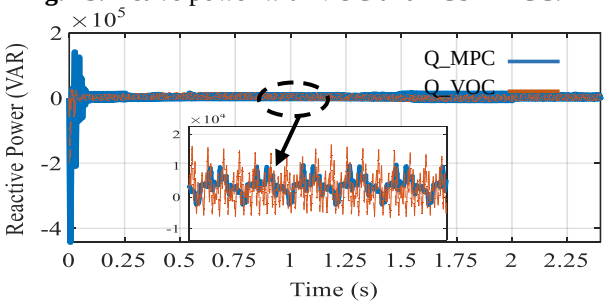

Fig. 14. Reactive power with VOC and FCS-MPCC.

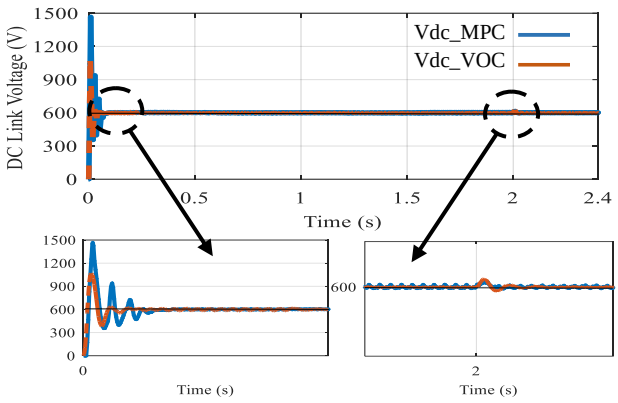

Fig. 15. DC voltage.

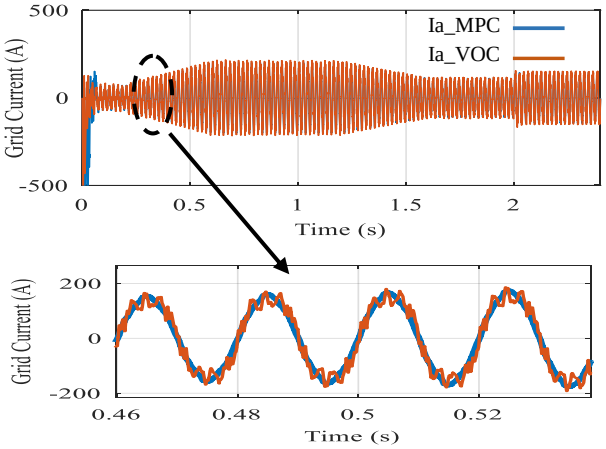

Fig. 16. Currents phase (a) with VOC and FCS-MPCC.

The total harmonic distortion (THD) of the grid current is less than that of electricity and the total harmonic distortion (THD) of the grid current is less than 5%. This enables us to meet grid connection requirements. A comparison of the THD of the network current shown in figures 17a and 17b shows that the THD of the current is 21.19% with the traditional decoupling PI control (VOC) to 4.43% with the FCS- MPCC system. Overall, the quality of the output waveforms is greatly improved, as is the accuracy.

We therefore conclude that the FCS-MPCC method considerably improves control stability, quality and accuracy.

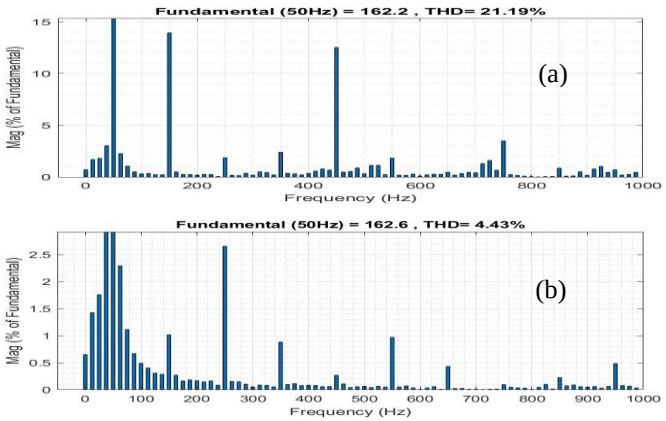

Fig. 17. Harmonic analysis of A-phase grid current:

a) THD of the VOC, b) is the THD of FCS- MPC.

6. Conclusion

The control approaches proposed in this study, namely (PSO) algorithm using a quadratic criterion-based objective function to track the global maximum power point of the photovoltaic generator, and the heuristic method of Finite Control Set Model Predictive Control Current (FCS-MPCC) for selecting the best combination of switching states for a three-level three-phase NPC inverter, have been shown to be effective in managing the active and reactive power of a photovoltaic solar system connected to a distribution grid, regardless of changes in irradiation levels. The analysis of the results displayed in blue represent the FCS-MPCC method, while those in red correspond to the VOC method. The FCS-MPCC reduces current THD, improves power quality and speeds up current processing. The result is lower current THD, better power quality, faster current tracking and improved dynamic performance compared to VOC control.

References

[1] M. S. Salvarli and H. Salvarli, “For sustainable development: Future trends in renewable energy and enabling technologies”, in Renewable Energy Resources, Challenges and Applications: Intech Open, 2020.

[2] Ch. Kavuma, D. Sandoval and K. J. D. Hakizimana, “Effect of distributed solar energy generation on Uganda’s electricity grid stability”, International Journal of Renewable Energy Research”, Vol 12, No 4, Dec. 2022.

[3] K. Chahine, M. Tarnini, N. Moubayed, and A. El Ghaly, “Power quality enhancement of grid-connected renewable systems using a matrix-pencil-based active power filter”, Sustainability, Vol. 15, No. 1, Jan. 2023.

[4] B. Hangun, O. Eyecioglu and M. Beken, “Forecasting the stability of a 4-node architecture smart grid using machine learning”, 10th International Conference on Smart Grid Istanbul, Turkey, pp.440-442, 2022.

[5] T. S. Genc and S. Kosempel, “Energy transition and the economy: A review article”, Canada, Energies MDPI, Vol. 16, No. 7, 2965 March 2023.

[6] A. E. Ghaly, M. Tarnini, N. Moubayed, and K. Chahine, “Hybrid active power filter using a filter-less extraction technique”, in 2022 11th International Conference on Renewable Energy Research and Application (ICRERA), Istanbul, Turkey: IEEE, pp. 452– 454, September 2022.

[7] E. Ö. Yüzer, “A review of the development of solar energy capacity in Turkey”, 1st International Conference on Modern and Advanced Research, Konya, Turkey, July 2023.

[8] M. Irfan, Z.Y. Zhao, M. Ahmad, M. C. Mukeshimana, “Solar energy development in Pakistan: barriers and policy recommendations”, Sustainability, https://doi.org/10.3390/su11041206, 2019.

[9] T. Brahim, A. Jemni, "Economical assessment and applications of photovoltaic/thermal hybrid solar technology: A review", in Solar Energy, Vol 153, pp 540-561, 2017.

[10] K. Arulkumar, K. Palanisamy, D. Vijayakumar, "Recent advances and control techniques in grid connected PV system – A review", in Vellore. Vol 6, No 3, 2016.

[11] F. Ayadi, I. Colak, I. Garip, and H. I. Bulbul. "Impacts of renewable energy resources in smart grid", In 2020 8th International Conference on Smart Grid (icSmartGrid), pp. 183-188. IEEE, June 2020.

[12] M. Yasir, A. Khan, H. Liu, Z. Yang, X. Yuan, "A Comprehensive review on grid connected photovoltaic inverters, their modulation techniques, and control strategies, review", Energies, 2020.

[13] A. Belkaid, K. Kayisli, I. Colak, S. Hadji and O. Guenounou, "Smart power conditioning unit utilizing enhanced inc-con MPPT for photovoltaic power plants", Internatıonal Journal of Smart Grid, Vol.8, No.1, March, 2024.

[14] W. A. Abri, R. A. Abri, H. Yousef and A. Al-Hinai, "A global MPPT based on bald eagle search technique for PV system operating under partial shading conditions", 10th International Conference on Smart Grid (icSmartGrid), Istanbul, Turkey, pp. 325-332, 2022.

[15] F. Tahiri, A. Harrouz, I. Colak, M. A. Hartani, F. Bekraoui and I. Boussaid, "Comparative study of the MPPT methods applied to the PV system; Perturbation & Observation technique, sliding mode control and fuzzy logic control", Conference: 11th International Conference on Smart Grid June 2023.

[16] P. Roy, J. He, T. Zhao and Y. V. Singh, "Recent advances of wind solar hybrid renewable energy systems for power generation: a review", in IEEE Open Journal of the Industrial Electronics Society, vol. 3, pp. 81-104, January 2022.

[17] R. Z. Caglayan, K Kayisli, M Roscia, A Harrouz, A Nasri, "A Comparative Analysis of P&O, IC and Super twisting sliding mode based MPPT methods for PV and fuel cell sourced hybrid system", International Journal of Renewable Energy Research, vol.13, no.3, September, 2023.

[18] N. P. Bishnu, I. Sayemul, A. K. Podder, "MPPT methods for solar PV system: a simulation-based comparative analysis", Conference: 5th International Conference on Electrical Information and Communication Technology (EICT), Khulna, Bangladesh IEEE, 17-19 Dec 2021.

[19] H. M. Abd Alhussain, N. Yasin, "Modeling and simulation of solar PV module for comparison of two MPPT algorithms (P&O & INC) in MATLAB/Simulink'', Indonesian Journal of Electrical Engineering and Computer Science in Baghdad, Iraq., ISSN: 2502 -4752, Vol 18, No. 2, pp. 666–677, 2020.

[20] R. Aljarrah, M. S. Ayaz, Q. Salem, M. Al-Omary, I. Abuishmais, W. AlRousan, "Application of passive harmonic filters in power distribution system with high share of PV systems and non-linear loads", International Journal of Renewable Energy Research, vol. 13, no. 1, pp. 401-411, March 2023.

[21] M. Ahmed, I. Harbi, R. Kennel, J. Rodríguez, M. Abdelrahem, "Evaluation of the main control strategies for grid-connected PV Systems", Advanced Control Techniques for Renewable Energy Systems and Power Electronics Vol. 2, Sustainability 14, 11142.

[22] J. B. Sahu, B. Nayak and S. Choudhury, "Power tracking capability enhancement of a grid tied partially shaded photovoltaic system through MPC Based maximum power point technique", International Journal of Renewable Energy Research, Vol.12, No.2, 2022.

[23] P. Marthi, S. Debnath and J. Choi, "Interpolation methods to enable fast and accurate EMT simulation of PV inverters", Nisantasi University. From IEEE Xplore on December 03, 2023.

[24] A. Seck, M. Thiam, M. Sarr, I. Ka and M. Wade, "Comparative study of photovoltaic models using simulation and experimental studies", International Journal of Renewable Energy Research, Vol. 12, No.4, December 2022.

[25] T. AlSkaif, S. Dev, L. Visser, M. Hossari, and W. van Sark, "A systematic analysis of meteorological variables for PV output power estimation", Renewable Energy, vol. 153, pp. 12–22, June. 2020.

[26] Z. Massaq, "Design of high–performance fuzzy–predictive controllers for a photovoltaic/battery pumping system", Internatıonal Journal of Renewable Energy Research, Vol.13, No.1, March, 2023.

[27] H. N. Kadeval and V. K. Patel, "Mathematical modelling for solar cell, panel and array for photovoltaic system", Journal of Applied and Natural Science, in India, vol 13, pp 937 – 943, 2021.

[28] M. R. Behiri, M. A. Mohamed, M. J. Al Shammri and H. Rezk, "Energy performance analysis of on-grid solar photovoltaic system a practical case study", Internatıonal Journal of Renewable Energy Research Vol.9, No.3, September 2019.

[29] N. Priyadarshi, A. K. Sharma and S. Priyam, "Practical realization of an improved photovoltaic grid integration with MPPT", Internatıonal Journal of Renewable Energy Research, Vol.7, No.4, 2017.

[30] A. A. Abd-Elaziz, S. M. Dabour and M. F. Elmorshedy, E. M. Rashad, "Application of FCS-MPC for split-source ınverter-based single-phase grid-connected PV systems", In Proceedings IEEE Conference on Power Electronics and Renewable Energy (CPERE), Luxor, Egypt, pp. 1–6, February 2023.

[31] M. Tarnini, Kh. I. Saab and A. El Ghaly, "A power electronic controller based algorithm for output power prediction of a PV panel", Internatıonal Journal of

Renewable Energy Research, Vol.13, No.3, September, 2023.

[32] Y. Izgheche, T. Bahi, "Maximum power point tracking control of photovoltaic system based on metaheuristic algorithm", 3rd International Conference on Engineering and Applied Natural Sciences, Turkey, Konya, 2023.

[33] S. Nyamathulla, D. Chittathuru, "A review of multilevel inverter topologies for grid-connected sustainable solar photovoltaic systems", Sustainability MDPI on September 2023.

[34] A. Lakhdari, B. Benlahbib, T. Abdelkrim, "Control for three-phase three-level NPC inverter based APF interfacing single stage photovoltaic system to the grid", Journal European des systems Automatisés, 55, 1, pp. 25–34, 2022.

[35] R. Pradhan, A. Panda, "Modeling and simulation of a MPC Based grid-tied PVDG system", International Journal of Renewable Energy Research, Vol.12, No 1, 2022. .